Retrieval of Reflectance From AVIRIS-Measured Radiance Using a Radiative Transfer Code

Robert O. Green

Jet Propulsion Laboratory
California Institute of Technology
Pasadena, California

Abstract. Calibrated radiance data measured by the Airborne Visible/Infrared Imaging Spectrometer (AVIRIS) are reduced to reflectance using a radiative transfer code. Reflectance is derived through compensation of the solar irradiance spectrum, solar-illumination geometry, atmospheric water vapor absorption, atmospheric scattering, absorption of the well-mixed gases, and an estimate of surface slope. Solar irradiance, illumination, and an atmospheric model are established from the location, season, and time of AVIRIS data acquisition. For each AVIRIS spatial resolution element, an estimate of total-column water vapor was derived directly from the AVIRIS radiance data. A retrieval of the surface-pressure elevation was generated from the 760-nm oxygen absorption band and the 2070-nm carbon-dioxide band measured within the AVIRIS spectrum. In situ measurements of atmospheric optical depths were used to constrain the atmospheric scattering properties at a point location. Scattering was extrapolated throughout the scene based upon the derived surface-pressure estimates. Absorption caused by well-mixed gases was constrained by the pressure elevation determinations. From the total-column water determination and an assumption of expected lateral homogeneity of water vapor over short distances, surface slopes were estimated for each spatial element. These parameters were used to constrain a radiative transfer code for retrieval of reflectance from AVIRIS measured radiance. The retrieval algorithm is evaluated with AVIRIS imagery acquired over a region where spectra of two surface targets have been independently acquired. The precision and accuracy of the retrieval algorithm are discussed.

1. Introduction

An algorithm to retrieve surface reflectance directly from AVIRIS-measured radiance using the LOWTRAN 7 (Kneizys et al., 1989) radiative transfer code is described.

AVIRIS measures the total upwelling radiance incident at the sensor with 224 spectral channels from 400 to 2450 nm in the electromagnetic spectrum. The spectral sampling interval and response function at full-width half-maximum (FWHM) throughput is nominally 10 nm. AVIRIS images are acquired with a width of 11 km and a length ranging from 10 to 100 km. The spatial resolution is nominally 20-by-20 m for all 224 spectral channels. The spectral as well as radiometric characteristics are determined for each channel during a laboratory calibration (Chrien et al., 1990a).

The AVIRIS data described here were acquired over the Clark Mountains, California, on July 23, 1990 at 20:20 universal coordinated time (UCT). These data were measured as part of an in-flight validation and calibration experiment undertaken to assess AVIRIS in-flight performance. Data were acquired over an occurrence of the

mineral bastnaesite, which possesses 12 strong absorption features (Adams, 1965) within the AVIRIS spectral range. These known absorptions allow confirmation of the in-flight spectral calibration of AVIRIS (Green et al., 1988). The region covered by this data set is approximately 11-by-40 km trending northwest along the eastern flank of the Clark Mountains. Figure 1 shows the coverage of these AVIRIS data, as well as the location of sites A, B, and C, where surface and atmospheric measurements were acquired.

Measurements from the onboard reference were used to modify the radiometric calibration of the in-flight measured radiance. Based on a preliminary analysis in the laboratory, the onboard calibrator is stable to 2% (Chrien, 1990b). To correct the in-flight data, a ratio for each channel was formed between the signal from the onboard reference at the time of the laboratory calibration to the signal at the time of the data acquisition. This ratio deviated from unity at the ±5% level. These correction factors were multiplied against the Clark Mountains radiance to place an improved radiometric calibration on the in-flight data.

Surface-reflectance spectra were acquired in conjunction with the AVIRIS data acquisition. A set of 16 reflectance spectra from a 50-by-50-m asphalt parking lot located at site A was measured. These spectra were acquired with a field spectrometer that has a spectral channel sampling interval and a response function FWHM of less than 5 nm. This high spectral resolution is required for valid convolution of the field-reflectance spectra to the 10-nm spectral characteristics of AVIRIS. In addition to the asphalt spectra, a spectrum of the mineral bastnaesite was acquired from a laboratory mineral sample. This spectrally distinct mineral occurs on the surface at site B in the Clark Mountains AVIRIS data set. Figure 2 shows the mean reflectance of the asphalt parking lot and the bastnaesite targets.

At site C, atmospheric optical depths were measured on July 23, 1990 in support of the AVIRIS spectral calibration and validation experiment. The solar radiometer used has 10 discrete spectral channels with 10-nm response function FWHM positioned at 370, 400, 440, 520, 610, 670, 780, 870, 940, and 1030 nm. These data were reduced to atmospherical optical depth with the Langley plot method (Kastner, 1985). The reduced optical depths were used to constrain the LOWTRAN 7 midlatitude summer atmospheric model for analysis of the AVIRIS radiance data. The resulting measured optical depths and corresponding modeled LOWTRAN 7 optical depths for site C are given in Figure 3.

2. Reflectance Retrieval Algorithm

An algorithm to retrieve reflectance directly from imaging-spectrometer-measured radiance using a radiative transfer code was originally developed for data acquired from the Airborne Imaging Spectrometer (AIS) (Conel et al., 1987). The method has since been augmented and used with AVIRIS data (Green et al., 1990a, and Green, 1990b). The algorithm presented here has been refined and expanded to maximize utilization of parameters derived directly from AVIRIS data for the retrieval of reflectance.

This algorithm treats the total upwelling radiance measured by AVIRIS for each spectral channel, L_t, as the combination of the two-way transmitted surface-reflected radiance, L_r, plus atmospheric path scattering radiance, L_p, as given in Equation 1.

$$L_t = L_r + L_p \quad (1)$$

The reflected radiance, L_r, is isolated in Equation 2 through subtraction of the path radiance component, L_p, from the total measured radiance, L_t. The path radiance is that radiance measured by AVIRIS derived solely from the atmosphere. The path radiance calculated with LOWTRAN 7 for an atmospheric model that is constrained by solar-illumination geometry, pressure elevation, water vapor absorption, atmospheric scattering, and well-mixed gas absorption is derived for each spatial resolution element.

$$L_r = L_t - L_p \quad (2)$$

The resulting AVIRIS-reflected radiance component is given in Equation 3, as the solar irradiance multiplied by the cosine of the solar zenith angle over pi steradians, $E_S\cos\theta/\pi$, which is multiplied by the downward atmospheric transmittance T_d, surface reflectance ρ, and upward atmospheric transmittance T_U.

$$L_r = [E_S\cos\theta/\pi]T_d\rho T_u \quad (3)$$

Using LOWTRAN 7, the reflected radiance for a 100% reflectance lambertian surface is calculated for the illumination and atmosphere determined for each AVIRIS spatial element, L_{r100}. The ratio of the AVIRIS-measured reflected radiance and the LOWTRAN 7 modeled 100% reflectance radiance is given in Equation 4.

$$L_r / L_{r100} = [E_S\cos\theta/\pi]T_d\rho T_u / [E_S\cos\theta/\pi]T_d\rho_{100}T_u \quad (4)$$

This ratio is solved for AVIRIS lambertian equivalent reflectance as in Equation 5.

$$\rho = (L_r/L_{r100})\rho_{100} \quad (5)$$

This approach of modeling the atmospheric path radiance and a known surface-reflected radiance for retrieval of reflectance is adopted because only limited modifications to existing radiative transfer codes such as LOWTRAN 7 are required for implementation.

3. Constraint of Radiative Transfer Code

Retrieval of reflectance from AVIRIS radiance with this algorithm requires the accurate constraint of the radiative transfer code of the atmosphere and illumination for each spatial resolution element.

The solar spectrum contained within the LOWTRAN 7 radiative transfer code is used as the exoatmospheric irradiance. Solar-illumination geometry is constrained by

the latitude, longitude, and time of the AVIRIS data acquisition over the Clark Mountains. A midlatitude, summer, and rural atmospheric model was used based on the location and season of data acquisition.

Total-column atmospheric water vapor is constrained based on a retrieval for each spatial element of the Clark Mountains AVIRIS data using the continuum interpolated band-ratio algorithm (Green et al., 1989). Accuracy of this algorithm has been established with respect to radiosonde and other spectroscopic water recoveries (Bruegge et al., 1990). Results from this retrieval are shown in Figure 4 [see slide 18] along with a composite image comprising three AVIRIS radiance channels. Retrieved water vapor amounts vary from 8 to 22 mm across the image. This extreme variability is driven largely by change in atmospheric path length as a function of surface elevation because water vapor absorbs strongly over much of the AVIRIS spectral range, an accurate estimate of water vapor is required for accurate reflectance retrieval. An error of 30% in estimation of atmospheric water vapor in the retrieval of reflectance may lead to errors of 10% in the retrieved reflectance (Green, 1989). In the future, a more robust inversion algorithm that applies a nonlinear least-squares approach with compensation for leaf water absorption (Green, 1991) will be used for the retrieval of atmospheric water vapor from AVIRIS radiance.

Optical depth measurements were acquired for constraint of atmospheric transmission and scattering characteristics at site C. These optical depths were extrapolated throughout the AVIRIS data set based on an estimate of the surface-pressure elevation. The pressure elevation was derived from the absorption of the 760-nm oxygen band measured within the AVIRIS spectrum. A continuum interpolated band ratio was calculated for this oxygen band for the Clark Mountains data set and was calibrated to surface-pressure elevation with LOWTRAN 7. For a single-resolution element, the precision of pressure element retrieval was determined as 12%. To improve the local precision with some loss of spatial resolution, a 9-by-9 spatial element filter was applied. An image of the retrieved pressure elevation is given in Figure 5 [see slide 19].

In addition to oxygen, the abundance of carbon dioxide was derived from the calibrated AVIRIS radiance using the 2070-nm absorption band. Again, a continuum interpolated band ratio calibrated through LOWTRAN 7 was used. An image of the retrieved carbon dioxide is given in Figure 6. This carbon dioxide retrieval also offers an estimate of surface-pressure elevation and is less influenced by atmospheric scattering.

Absorption of the well-mixed gases in the AVIRIS spectral range was varied based on the surface-pressure elevation. Ozone absorption was constrained based on the latitude and season of the AVIRIS acquisition.

An approach to estimating surface slope from the AVIRIS data set was investigated. This method requires precise retrievals of the water vapor from AVIRIS radiance and an assumption of expected lateral homogeneity of water vapor over short distances. From the Clark Mountains water vapor image, the equivalent surface elevations were calculated for each spatial element for the midlatitude summer atmospheric model with LOWTRAN 7. Estimates of the slope for each spatial element

were then calculated as the normal to a surface fit to the 3-by-3 encompassing spatial elements. A surface-slope correction image of the secant of the angle between the surface normal and the illumination direction is given in Figure 7. This slope correction image properly indicates a slope away from the illumination direction on the northern side of Clark Mountains. The validity of these slope estimates is a function of the dominance of topography in the modulation of water vapor abundance over the 3-by-3 spatial element regions. Further evaluation of this technique will require analysis with digital elevation data co-registered with the AVIRIS imagery.

4. Retrieval of Reflectance From AVIRIS Radiance

The reflectance retrieval algorithm constrained by the derived atmospheric characteristics was applied to the AVIRIS radiance imagery of the Clark Mountains. As an example of the radiance data, Figure 8 shows the measured radiance spectra for the asphalt and bastnaesite targets. Application of the retrieval algorithm resulted in the reflectance spectra given in Figure 9. For the asphalt target, the absolute agreement is good across the spectral range with an absence of evidence for uncompensated water vapor absorption or atmospheric scattering artifacts. The unique spectral features of the bastnaesite target in the 500 to 900 nm range are recovered accurately. Complete agreement between the laboratory and AVIRIS bastnaesite reflectance is not expected, based on the differing sampling scale of the laboratory and AVIRIS spectrometers. With the reduction of the AVIRIS radiance to reflectance analyses for the quantitative identification, assessment and monitoring of surface spectral reflectance characteristics become possible.

5. Error Discussion

The precision of the reflectance spectra retrieved through this algorithm relies on the precision of the AVIRIS-measured radiance and of the parameters used to constrain the radiative transfer code. Precision of the AVIRIS data and derived parameters is a function of the instrument performance, atmospheric characteristic, surface reflectance, and illumination geometry. Additional analyses are required to quantify the influence of these factors on the retrieved reflectance over the Clark Mountains.

Accuracy of the retrieval depends on the accuracy of AVIRIS spectral and radiometric calibration. For example, errors in the knowledge of the in-flight spectral characteristic of AVIRIS will cause significant errors in the retrieved reflectance. These errors result from the many strong absorptions present in terrestrial radiance spectra (Green et al., 1990a). Fortunately, uncertainty in the in-flight spectra characteristics of AVIRIS may be assessed and corrected based on the imaging spectrometer data themselves (Conel et al., 1987; Green et al., 1988; and Green et al., 1990a). Uncertainty in the absolute radiometric calibration of AVIRIS will introduce proportional uncertainty in retrieved reflectance. Efforts are ongoing to maintain, monitor, and improve the absolute calibration accuracy of AVIRIS (Chrien et al., 1990a, and Green et al., 1990a).

Accuracy of the radiative transfer code and model atmosphere directly influences the retrieved reflectance. Currently, the MODTRAN radiative transfer code

(Berk et al., 1989) is being evaluated as a potential improvement over LOWTRAN 7. MODTRAN operates at a higher spectral resolution and more accurately models water vapor absorption. Other radiative transfer codes that more fully treat atmospheric scattering and surface bidirectional reflectance are being examined as well.

The parameters used to constrain the radiative transfer code for reflectance retrieval directly affect the accuracy of the result. Ideally, all atmospheric and surface-slope parameters should be known for each AVIRIS spatial resolution element. In the absence of independent knowledge of these constraining parameters, algorithms for deriving estimates of these parameters from the AVIRIS radiance data have been developed. Validation of the accuracy of the retrievals of water vapor, oxygen, and carbon-dioxide abundance, as well as the parameters derived from these abundances, is essential to establishing the accuracy of the reflectance retrieval. Efforts are ongoing with in situ field validations and computational sensitivity analyses to determine these accuracies.

6. Conclusion

Reflectance spectra were successfully retrieved from calibrated AVIRIS radiance data using the LOWTRAN 7 radiative transfer code. This reflectance retrieval algorithm was constrained by parameters derived largely from the AVIRIS radiance data themselves. For the Clark Mountains AVIRIS data set, comparison of the AVIRIS retrieved reflectance and reflectance spectra from two surface sites showed consistent agreement. Work is required to further validate the accuracy of the derived constraining parameters and of the retrieved surface reflectance over a range of atmospheric and surface conditions. As presented, this algorithm provides an approach for the routine retrieval of reflectance from imaging-spectrometer-measured radiance. Retrieval of reflectance is essential for the quantitative investigation of surface composition, for the comparison of surfaces from one region to another, and for the study of surfaces and surface processes through time.

Acknowledgment

This research was carried out at the Jet Propulsion Laboratory, California Institute of Technology, under contract with the National Aeronautics and Space Administration.

References

Adams, J.W., "The visible region absorption spectra of rare-earth minerals," *The Amer. Min.*, 50, 356-367, 1965.

Berk, A., L.S. Bernstein, and D.C. Roberson, *MODTRAN: A Moderate Resolution Model for LOWTRAN 7*, U.S. Air Force Geophysical Laboratory (AFGL), Hanscom Air Force Base, Massachusetts, 1989.

Bruegge, C.J., J.E. Conel, J.S. Margolis, R.O. Green, G. Toon, V. Carrere, R.G. Holm, and G. Hoover, "In situ atmospheric water vapor retrieval in support of AVIRIS validation," *Imaging Spectroscopy of the Terrestrial Environment*, SPIE Vol. 1298, 1990 (in press).

Chrien, T.G., R.O. Green, and M. Eastwood, "Laboratory spectral and radiometric calibration of the Airborne Visible/Infrared Imaging Spectrometer (AVIRIS)," *Imaging Spectroscopy of the Terrestrial Environment*, SPIE Vol. 1298, 1990a (in press).

Chrien, T.G., personal communication, Jet Propulsion Laboratory, Pasadena, California, 1990b.

Conel, J.E., R.O. Green, G. Vane, C.J. Bruegge, R.E. Alley, and B.J. Curtiss, "AIS-2 Radiometry and A Comparison of Methods for the Recovery of Ground Reflectance," *Proceedings of the Third Airborne Imaging Spectrometer Data Analysis Workshop*, (G. Vane, ed.), JPL Publication 87-30, Jet Propulsion Laboratory, Pasadena, California, 1987.

Conel, J.E., R.O. Green, V. Carrere, J.S. Margolis, R.E. Alley, G. Vane, C.J. Bruegge, and B.L. Gary, "Atmospheric Water Mapping with the Airborne Visible/Infrared Imaging Spectrometer (AVIRIS), Mountain Pass, California," *Proceedings of the Airborne Visible/Infrared Imaging Spectrometer (AVIRIS) Performance Evaluation Workshop,* (G. Vane, ed.),.JPL Publication 88-38, Jet Propulsion Laboratory, Pasadena, California, pp. 21-26, 1988.

Green, R.O., G. Vane, and J.E. Conel, "Determination of Aspects of the In-Flight Spectral, Radiometric, Spatial and Signal-to-Noise Performance of the Airborne Visible/Infrared Imaging Spectrometer Over Mountain Pass, California," *Proceedings of the Airborne Visible/Infrared Imaging Spectrometer (AVIRIS) Performance Evaluation Workshop*, (G. Vane, ed.), JPL Publication 88-38, Jet Propulsion Laboratory, Pasadena, California, pp. 162-184, 1988.

Green, R.O., V. Carrere, and J.E. Conel, "Measurement of atmospheric water vapor using the Airborne Visible/Infrared Imaging Spectrometer," *Image Processing '89,* American Society for Photogrammetry and Remote Sensing (ASPRS), 1989.

Green, R.O., J.E. Conel, J.S. Margolis, V. Carrere, C.J. Bruegge, and G. Hoover, "Determination of the In-Flight Spectral and Radiometric Characteristics of the Airborne Visible/Infrared Imaging Spectrometer (AVIRIS)," *Proceedings of the Second Airborne Visible/Infrared Imaging Spectrometer (AVIRIS) Workshop*, JPL Publication 90-54, Jet Propulsion Laboratory, Pasadena, California, 1990a.

Green, R.O., "Retrieval of Reflectance from Calibrated AVIRIS Radiance for Lithological Mapping of the Clark Mountains, California," *Proceedings of the Second Airborne Visible/Infrared Imaging Spectrometer (AVIRIS) Workshop*, JPL Publication 90-54, Jet Propulsion Laboratory, Pasadena, California, 1990b.

Green, R.O., J. E. Conel, J. Margolis, C. Bruegge, and G. Hoover, "An Inversion Algorithm for Retrieval of Atmospheric and Leaf Water Absorption from AVIRIS Radiance with Compensation for Atmospheric Scattering," *Proceedings of the Third Airborne Visible/Infrared Imaging Spectrometer (AVIRIS) Workshop*, JPL Publication 91-28, Jet Propulsion Laboratory, Pasadena, California, 1991 (this publication).

Kastner, C.J. (now Bruegge, C.J.), "In-flight absolute radiometric calibration of the Landsat Thematic Mapper," a Ph.D. Dissertation, University of Arizona, 1985.

Kneizys, F.X., E.P. Shettle, G.P. Anderson, L.W. Abrew, J.H. Chetwynd, J.E.A. Shelby, and W.O. Gallery, *Atmospheric Transmittance/Radiance: Computer Code LOWTRAN 7*, U.S. Air Force Geophysical Laboratory (AFGL), Hanscom Air Force Base, Massachusetts, 1989.

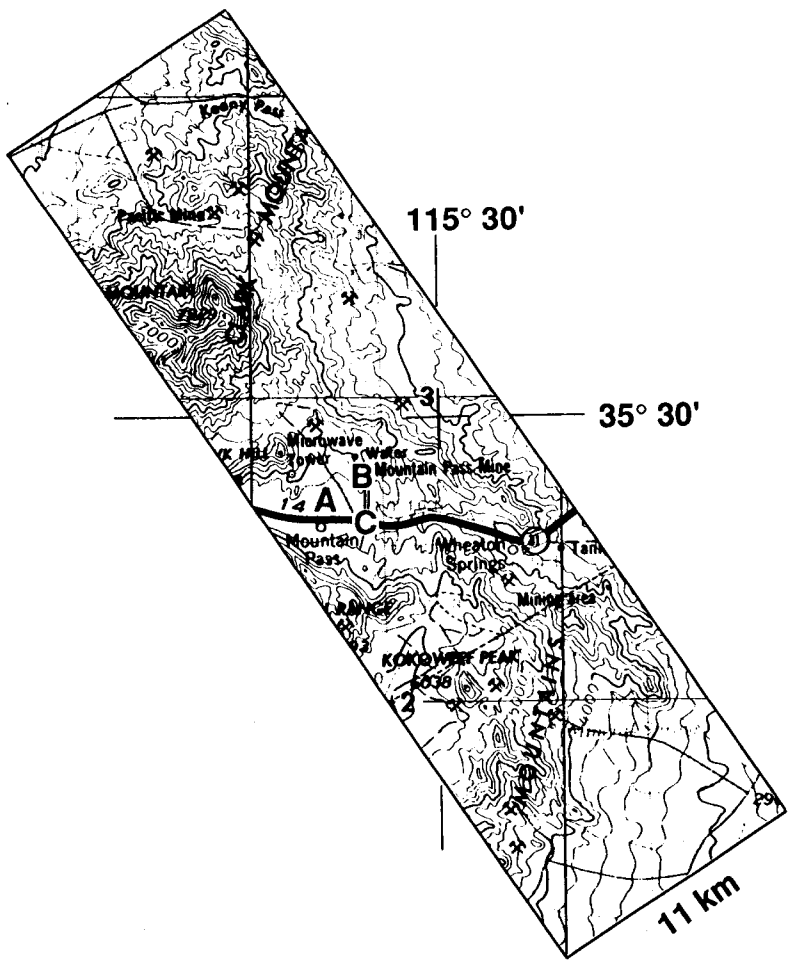

Figure 1. Location of the AVIRIS data set for the Clark Mountains, California. The targets A, B, and C, corresponding to an asphalt parking lot, bastnaesite mineral site, and atmospheric measurement site, are shown as well.

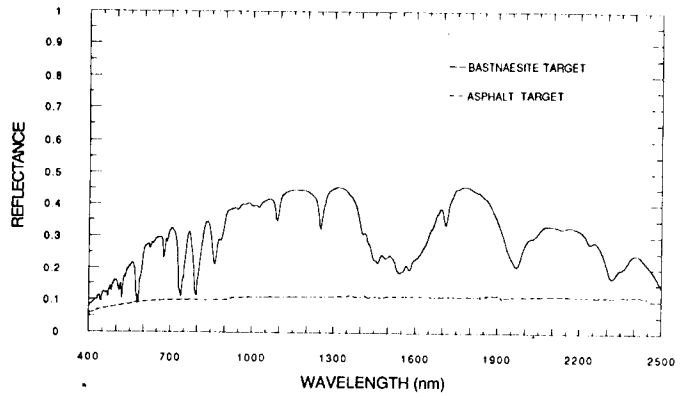

Figure 2. Reflectance of the asphalt target resulting from the mean of 16 in situ field spectra and the laboratory reflectance spectrum of the mineral bastnaesite.

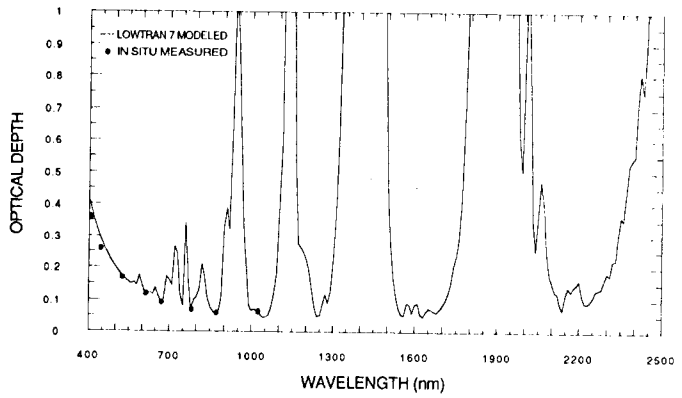

Figure 3. Discrete optical depths calculated from sun photometer measurements acquired adjacent to site A on the day of the AVIRIS overflight. The contiguous LOWTRAN 7 modeled optical depths determined to correspond to the measured discrete optical depths are also given.

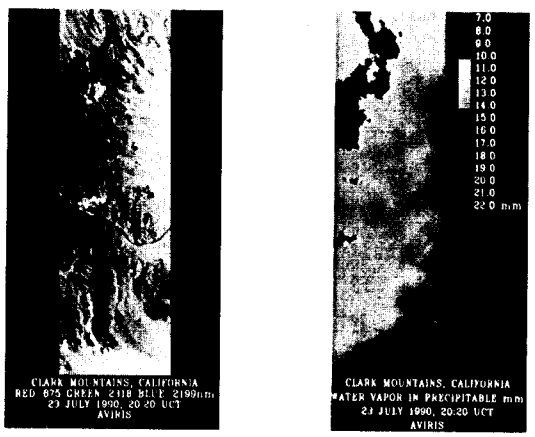

Figure 4. AVIRIS radiance image of the Clark Mountains scene on the left, and the total-column water vapor retrieved for that scene on the right. The water vapor varies from 8 to 22 mm of precipitable water within this 11- by-40-km region. [See slide 18].

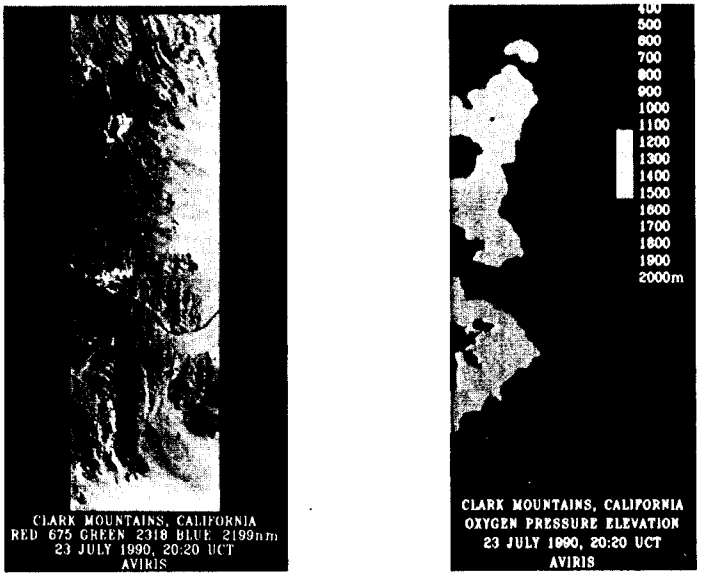

Figure 5. Surface-pressure elevation derived from the absorption of the 760-nm oxygen absorption band measured within the AVIRIS spectrum on the right. AVIRIS radiance image of the Clark Mountains scene on the left. [See slide 19.]

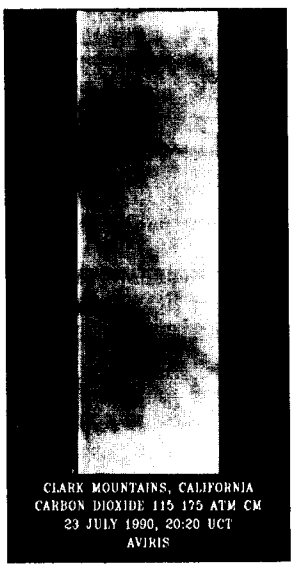

Figure 6. Retrieved carbon-dioxide abundance image from calibrated AVIRIS radiance data using the 2070-nm absorption band.

Figure 7. Estimation of surface slope through calculation of local relative elevations derived from water vapor retrieval.

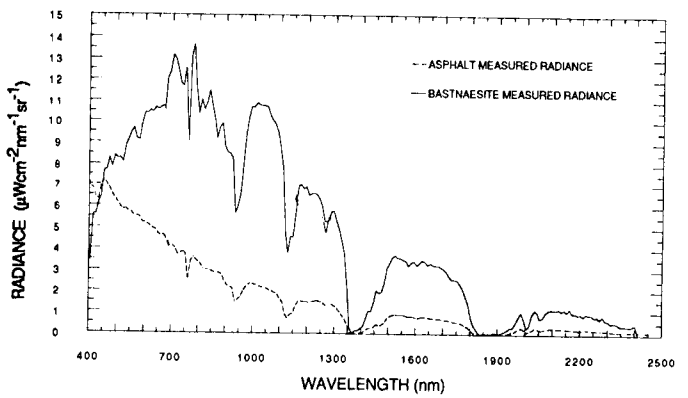

Figure 8. AVIRIS-calibrated radiance spectrum for the asphalt target and the bastnaesite target.

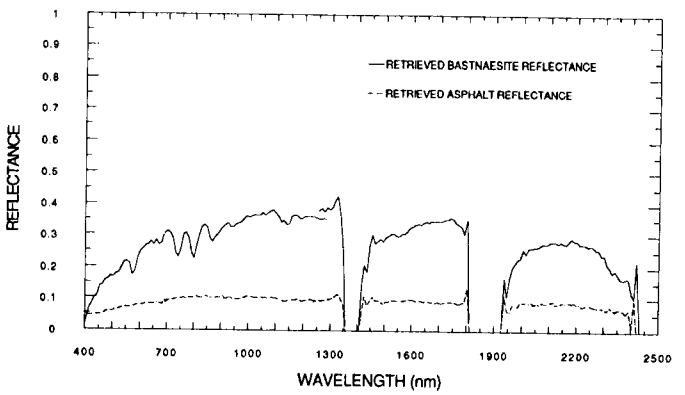

Figure 9. AVIRIS-retrieved reflectance for the asphalt target and the bastnaesite target.